Biased Estimation of Antenna Radiation Efficiency Within Reverberation Chambers Due to Unstirred Field: Role of Antenna Stirring

Wafa Krouka, Francois Sarrazin, Jérôme Sol, Philippe Besnier, Elodie Richalot

HAL Id: hal-03665327

https://hal.science/hal-03665327

Submitted on 11 May 2022

Biased Estimation of Antenna Radiation Efficiency Within Reverberation Chambers Due to Unstirred Field: Role of Antenna Stirring

Wafa Krouka, François Sarrazin, Jérôme Sol, Philippe Besnier, *Senior Member, IEEE* and Elodie Richalot, *Member, IEEE*

Abstract—Reverberation chambers (RCs) are now a reliable alternative to anechoic chambers to perform antenna radiation efficiency measurements. Most methods, including the two-antenna one used in this paper, are based on the evaluation of the stirred components of the scattering parameters. They are obtained by subtracting the average scattering parameters from the measured ones. This averaging is performed thanks to mechanical stirring, that is sometimes supplemented by additional stirring such as antenna stirring (which includes platform stirring and source stirring). In this paper, we present an extensive study on the role of antenna stirring in the retrieved radiation efficiency. Four measurement campaigns were successively performed: without antenna stirring, with platform stirring only, with source stirring only, and with a combined stirring of both antennas. Performing only source stirring or platform stirring leads to a biased estimation of the radiation efficiency. Therefore, we showed that the stirring of both antennas is mandatory in order to obtain an unbiased estimation of the radiation efficiency.

Index Terms—antenna characterization, antenna stirring, efficiency measurement, mode-stirring, platform stirring, radiation efficiency, reverberation chamber, source stirring, unstirred energy

I. INTRODUCTION

BESIDE the enthusiasm for the millimeter wave spectrum regarding the ultra-high data-rate race [1], the 5G system also gives prominence to the sub-6 GHz bands [2] mainly through Internet-of-Things applications. The need for low-power, low-profile and low-cost 5G devices leads to new challenges regarding antenna design where a reduced bandwidth is often targeted in order to keep the device miniature [3], [4]. Therefore, the antenna radiation efficiency becomes the most important metric as it is crucial to manage the energy consumption of the device. In addition to the antenna design challenges, there is a need for fast, reliable and low-cost characterization techniques of such small 5G devices.

Antenna radiation efficiency is defined as the ratio between the radiated power and the incident power at the antenna port [5]. Its evaluation can be performed by various means,

including within an anechoic chamber (AC) using the gain-integration technique, or using a Wheeler cap [6] or its ultra-wide band extension [7]. For many years now, reverberation chambers (RCs) have become popular for antenna radiation efficiency measurement as they avoid some constraints usually experienced during AC measurements such as the antenna under test (AUT) accurate positioning and alignment during its rotation, while controlling the measurement uncertainties [8]. Several techniques have been proposed to measure the antenna radiation efficiency in an RC [9]–[14]. Among them, the one introduced by Holloway [12] in 2012 is one of the most popular and well established, especially as it avoids the use of a reference antenna with known efficiency. The method is based on the difference between the RC Q-factors estimated in the time and the frequency domains, the first one being independent of antenna radiation efficiencies. Three variants are introduced in [12], namely the one-, the two- and the three-antenna methods. In this paper, the two-antenna method is used as it offers an interesting trade-off between the high-uncertainty one-antenna method and the time-consuming three-antenna method.

Measurement uncertainties mainly rely on the stirring process, that aims at ensuring a sufficient number of uncorrelated RC configurations. The mode stirring within an RC is usually ensured by one or two rotating metallic stirrers, however, other types of stirring have been suggested in the literature [15]. Source-stirred chambers have been widely studied and are based on a source variation either by moving one source within the cavity — manually [16] or with a robotic arm [17] — or by using arrays of successively-fed antennas [18]. It is shown that source stirring can be a good alternative to the classical mechanical stirring [19]. If the different sources are oriented orthogonally to each other, different polarizations are considered and this technique is therefore referred to as polarization stirring [20]. Platform stirring has also been suggested for antenna radiation efficiency measurement [21]. It aims at rotating the AUT over a platform in order to avoid direct coupling with the source antenna [22]. Platform stirring has also been successfully used to perform accurate antenna reflection coefficient measurements within an RC [23].

It has been shown that the two-antenna method leads to accurate and repeatable measurement of antenna radiation efficiency [24], [25] with limitations when dealing with highly-mismatched or high-loss antennas such as a narrowband ones [26]. However, we will show that such method is very sen-

sitive to the evaluation of the stirred components of the S-parameters. S-parameters measured within an RC depend on both the considered antennas and the scattering environment provided by the RC. They combine contributions from the stirred energy (i.e., the energy that interacts with the mode stirrer) and the unstirred energy (the energy that does not interact with the mode stirrer, including line-of-sight (LOS) and non-LOS energy), so that they can be written as:

$$S_{ii} = S_{ii,\mathrm{us}} + S_{ii,\mathrm{s}} \tag{1}$$

where $S_{ii,\mathrm{us}}$ and $S_{ii,\mathrm{s}}$ are the unstirred and the stirred component of S_{ii}, respectively. It is usually assumed that, for an infinite number of uncorrelated RC configurations, the average of the reflection coefficient over the stirring process $\langle S_{ii} \rangle$ converges towards the free-space (FS) reflection coefficient $S_{ii,\mathrm{FS}}$, i.e., the one that would be measured within an AC [27]. However, the measured unstirred energy is not only due to the FS component of the reflection coefficient but also to the direct paths between the antenna and the RC walls that do not interact with the mechanical stirrer. As we will see, this unstirred energy leads to a biased estimation of the antenna radiation efficiency.

Discrepancies (5% to 10%) have already been observed between comparative radiation efficiency measurements of the same antenna within two different RCs [28] and they have been attributed to the overall uncertainty budget. Indeed, a detailed uncertainty analysis of the two-antenna method [12] has shown up to 9% uncertainties for a similar setup. However, we show in this paper that discrepancies can also be attributed to systematic errors that arise due to residual unstirred components. In particular, we perform for the first time a study on the dependency of the estimated radiation efficiency on the unstirred energy in the RC. "Antenna stirring", i.e., the modification of the location and polarization of one or both antennas within the RC is performed to highlight this dependency. Please note that "antenna stirring" refers here to either or both "platform stirring" and "source stirring"; the former referring to the AUT stirring only and the latter referring to the measurement antenna stirring (different from the AUT). Antenna stirring is often seen as an additional stirring technique in order to obtain extra uncorrelated configurations. However, we will show here that it is also a way to decrease the unstirred components of the measured scattering parameters. As the radiation efficiency of the two antennas can be estimated with the same setup using the two-antenna method, both antennas are here alternately considered as the AUT and the measurement antenna, and thus both antennas are used to perform either the platform stirring or the source stirring.

Section II briefly recalls the two-antenna method and the parameters that need to be estimated. It also introduces the unstirred components in the scattering parameters model within an RC. After a presentation of the measurement setup, Section III presents the radiation efficiency estimation of both antennas, obtained after performing a stirring using the first antenna (Section III-B), the second antenna (Section III-C), and then a combined stirring of both antennas (Section III-D).

A summary of the impact of the different antenna-stirring approaches is then presented before concluding this paper.

II. MEASUREMENT METHOD AND MODEL

A. Measurement Method

We present in this Section a brief recall of the two-antenna method introduced in [12] and used in this paper for antenna efficiency measurements. Let us consider two antennas, namely A1 and A2, located within the working volume of an RC, and connected respectively to port 1 and port 2 of a VNA. The radiation efficiency of the ith antenna $\eta_{\mathrm{rad},i}$ can be computed as:

$$\eta_{\mathrm{rad},i} = \sqrt{\frac{\langle |S_{ii,\mathrm{s}}|^2 \rangle}{(1 - |\langle S_{ii} \rangle|^2)^2} \frac{V}{Q_{\mathrm{TD}}\, e_{\mathrm{b}}} \frac{16\pi^2}{\lambda^3}} \tag{2}$$

with $i = \{1, 2\}$, Q_{TD} the time-domain Q-factor, $S_{ii,\mathrm{s}}$ the stirred component of the S_{ii} parameter, e_{b} the enhanced backscatter coefficient, V the chamber volume, λ the wavelength, and $\langle \cdot \rangle$ denotes the ensemble average. The e_{b} parameter being itself dependent on $\langle |S_{ii,\mathrm{s}}|^2 \rangle$, it can be substituted by its expression (from (25) in [12]), it comes:

$$\eta_{\mathrm{rad},i} = \sqrt{\frac{\langle |S_{ij,\mathrm{s}}|^2 \rangle}{(1 - |\langle S_{ii} \rangle|^2)^2} \sqrt{\frac{\langle |S_{ii,\mathrm{s}}|^2 \rangle}{\langle |S_{jj,\mathrm{s}}|^2 \rangle}} \frac{V}{Q_{\mathrm{TD}}} \frac{16\pi^2}{\lambda^3}} \tag{3}$$

with $i = \{1, 2\}$, $j = \{1, 2\}$ and $i \neq j$. Therefore, the radiation efficiency estimation of the ith antenna is based on the estimation of 5 parameters:

- the stirred energy contribution of S_{ii},
- the stirred energy contribution of S_{jj},
- the stirred energy contribution of S_{ij},
- the time-domain Q-factor: Q_{TD},
- the squared modulus of the average of the AUT reflection coefficient: $|\langle S_{ii} \rangle|^2$.

We will see in Section III that the evaluation of the stirred components of the S-parameters is highly sensitive to the stirring process. An analytical model for the S-parameters measured within an RC is presented in Section II-B.

B. Antenna Reflection Coefficient Within an RC

An analytical model for an antenna reflection coefficient within an RC has been introduced in [29]:

$$S_{ii}(\alpha, p_i) = S_{ii,\mathrm{FS}} + \left(1 - |S_{ii,\mathrm{FS}}|^2\right) \eta_{\mathrm{rad},i} H_{ii}(\alpha, p_i) \tag{4}$$

where α is the stirrer angular position, p_i is the position of the ith antenna, $S_{ii,\mathrm{FS}}$ is the free-space (FS) component of the S_{ii} parameter, $\eta_{\mathrm{rad},i}$ is the radiation efficiency of the ith antenna, and $H_{ii}(\alpha, p_i)$ is the complex RC transfer function. Assuming a perfectly diffuse field, both real and imaginary parts of $H_{ii}(\alpha, p_i)$ are described by random variables following a centred Gaussian distribution. For an infinite number of uncorrelated configurations, we can assume that $\langle H_{ii}(\alpha) \rangle_\alpha = 0$ so that $\langle S_{ii}(\alpha) \rangle_\alpha = S_{ii,\mathrm{FS}}$. However, the unstirred component is not strictly equivalent to $S_{ii,\mathrm{FS}}$ as specular reflections that are, by definition, not stirred by the mode stirrer, also exist within

the RC. Therefore, the previous equation should be re-written as [30]–[32]:

$$S_{ii}(\alpha, p_i) = S_{ii,\text{FS}} +$$
$$\left(1 - |S_{ii,\text{FS}}|^2\right)\eta_{\text{rad},i} \times [H_{ii}(\alpha, p_i) + h_{ii}(p_i)] \quad (5)$$

where $h_{ii}(p_i)$ is the RC transfer function that accounts for LOS and/or specular reflections from the RC walls, and other standing objects within the RC towards the antenna. $h_{ii}(p_i)$ depends on the antenna position but, contrary to $H_{ii}(\alpha, p_i)$, it can not be described, according to stirrer positions α, by random variables following a centred Gaussian distribution. Indeed, a conventional mechanical stirring is only effective in decreasing $H_{ii}(\alpha, p_i)$ but won't modify $h_{ii}(p_i)$. Therefore, the unstirred component introduced in (1) can be expressed as:

$$S_{ii,\text{us}}(p_i) = S_{ii,\text{FS}} + \left(1 - |S_{ii,\text{FS}}|^2\right)\eta_{\text{rad},i} \times h_{ii}(p_i) \quad (6)$$

The last equation highlights the need to perform additional stirring such as platform stirring or source stirring in order to eliminate $h_{ii}(p_i)$. Please note that (5) can be generalized to the transmission coefficient as:

$$S_{ij}(\alpha, p_i, p_j) = S_{ij,\text{FS}} +$$
$$\sqrt{\left(1 - |S_{ii,\text{FS}}|^2\right)\left(1 - |S_{jj,\text{FS}}|^2\right)} \times$$
$$\sqrt{\eta_{\text{rad},i}}\sqrt{\eta_{\text{rad},j}} \times [H_{ij}(\alpha, p_i, p_j) + h_{ij}(p_i, p_j)] \quad (7)$$

It is emphasized that although S_{21} is sometimes referred as an RC transfer function in the literature, H_{12} is closer to the intrinsic transfer function of an RC as it does not depend on antenna parameters (matching and radiation efficiency).

III. MEASUREMENT RESULTS

A. Measurement Setup

All the experiments have been performed in the RC located at the ESYCOM laboratory, presented in Fig 1, whose dimensions are $2.95 \times 2.75 \times 2.35$ m^3. The RC has one vertical metallic stirrer to ensure the mechanical stirring over 72 stirrer positions. Two antennas, namely A1 and A2, are positioned within the RC and connected to port 1 and port 2 of a Rhode&Schwarz ZNB20 VNA, respectively. A2 is a wideband omni-directional antenna based on a half-disc slot excited by a microstrip monopole (Fig. 2 (left)) whereas A1 is a directional log-periodic antenna Schwarzbeck VUSLP 9111-400 (Fig. 2 (right)). S-parameters are measured in the 1.6 to 3 GHz frequency range, where the two antennas are well matched, with an IF BW of 1 kHz and 100 kHz frequency spacing. Antenna A2 is located on top of a rotating mast, 70 cm away from the rotation center, tilted by 45°, and 12 uniformly-distributed positions are considered over a revolution in order to perform the "A2 stirring". 12 positions of antenna A1 are also considered ("A1 stirring"). A1 is manually moved over 3 locations and 4 heights for each location, and its polarization is modified for each position. It is kept oriented towards the mechanical stirrer for all positions, in order to avoid direct coupling between the two antennas (A1 is never oriented towards A2). The effective number of uncorrelated
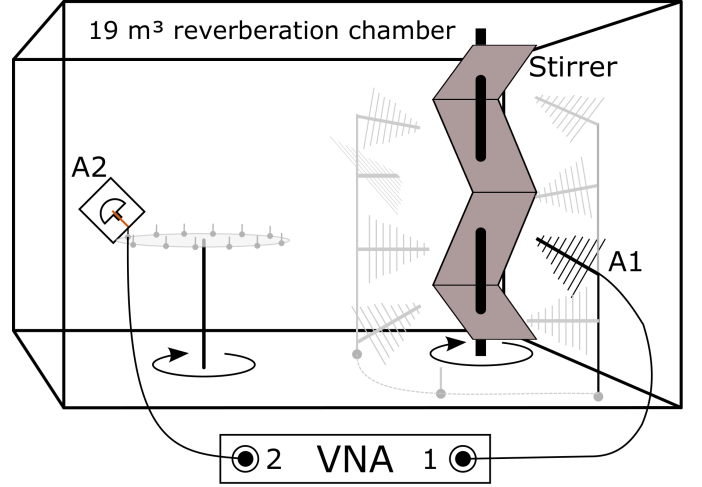

Fig. 1. Measurement setup within a 19 m^3 RC equipped with a mechanical stirrer. A2 is a wide-band slot antenna located on top of a rotating mast tilted by 45° (12 positions considered), and A2 is a log-periodic antenna oriented towards the mechanical stirrer, manually moved over 12 positions with various orientations.

Fig. 2. Pictures of the two antennas under test: the wide-band slot antenna A2 (left) and the log-periodic antenna A1 (right).

configurations N_{eff} provided by the mechanical mode-stirrer is estimated at 25 around the central frequency, according to [33].

Three different experiments are made in the following: 1) A2 stirring (Section III-B): A1 is kept fixed whereas the 12 positions of A2 are considered, 2) A1 stirring (Section III-C): A2 is kept fixed whereas the 12 positions of A1 are considered, and 3) Combined A1 and A2 stirring (Section III-D): both A1 and A2 are moved together over 12 positions each. It is emphasized that the number of stirrer and antenna positions (respectively 72 and 12) is kept constant for all the three experiments in order to provide a fair comparison between the stirring techniques. It takes approximately 10 minutes to perform a stirrer rotation (72 measurements) for one antenna configuration; therefore 2 hours are required to perform each set of measurement (12 antenna positions).

The enhanced backscattering constant e_b has been computed for all 36 measurements (12 antenna positions for each of the three experiments). It exhibits an average value of 2.16 (close to the ideal value of 2), with limited fluctuations (standard deviation averaged over the frequency bandwidth equal to 0.0617), therefore demonstrating its good spatial uniformity
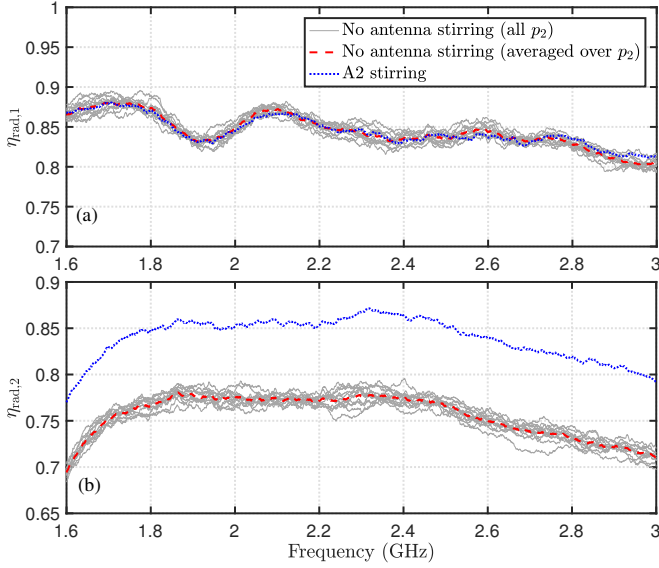
Fig. 3. Radiation efficiency of A1 (a) and A2 (b) as a function of frequency, with and without A2 stirring.

as required to apply the two-antenna method [12], [34].

B. A2 Stirring

In this part, we consider A1 fixed at one position whereas A2 is moved over the 12 considered positions. The radiation efficiencies of A1 and A2 are then computed according to the two-antenna method using (3), and presented respectively in Fig. 3(a) and Fig. 3(b) as a function of frequency. Two different cases have been considered regarding the computation of all the S-parameters: 1) Without A2 stirring: the S-parameters are averaged over all the mechanical stirrer positions and computed for each A2 position p_2 (solid grey curves); these 12 results are then averaged (dashed red curve), and 2) With A2 stirring: S-parameters are averaged over all the mechanical stirrer positions and A2 positions (dotted blue curve).

The A1 radiation efficiency (Fig. 3(a)) is estimated to be $85 \pm 5\%$ over the frequency range. Estimations for all p_2 positions are very consistent (normalized standard deviation of 78×10^{-4}) and the mean value is very similar to the one obtained using both mechanical and A2 stirring. It shows that the A2 stirring has almost no impact on $\eta_{\mathrm{rad},1}$. On the other hand, the A2 radiation efficiency exhibits a totally different behavior regarding the stirring process (Fig. 3(b)). Without A2 stirring, the radiation efficiency is estimated up to 78% in the 1.8 to 2.4 GHz frequency range, and all estimations are consistent (normalized standard deviation of 90×10^{-4}). However, once A2 stirring is performed, the radiation efficiency increases by 8% on average.

In order to determine the origin of such increase, the different parameters of (3), listed in Section II-A, are analyzed. As for the radiation efficiency, each parameter is computed with and without performing A2 stirring. The Q-factor is presented in Fig. 4 as a function of frequency. Its value increases from 6800 to 11000 over the frequency range and we can see that the additional stirring provided by the
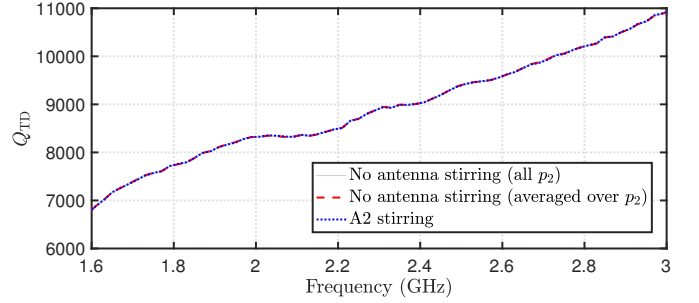

Fig. 4. RC Q-factor estimated in the time domain as a function of frequency, with and without A2 stirring.
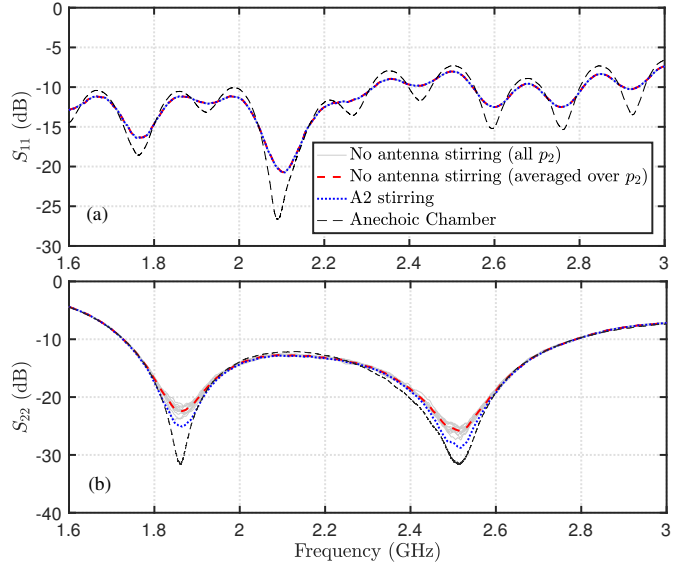

Fig. 5. Reflection coefficient of A1 (a) and A2 (b) as a function of frequency with and without A2 stirring. Results in RC are smoothed using a 100 MHz sliding window.

A2 movement does not induce a significant change in the estimated Q-factor. We define R_Q as the ratio of the Q-factor estimated using $\langle\langle|S_{21}(\alpha, p_2) - \langle\langle S_{21}(\alpha, p_2)\rangle_\alpha\rangle_{p_2}|^2\rangle_\alpha\rangle_{p_2}$ to the one estimated using $\langle\langle|S_{21}(\alpha, p_2) - \langle S_{21}(\alpha, p_2)\rangle_\alpha|^2\rangle_\alpha\rangle_{p_2}$ averaged over the frequency bandwidth. It is equal to 1.000 in this case (Table I) confirming the almost null impact of A2 stirring on the estimation of this parameter. The average reflection coefficients of both antennas are presented in Fig 5 and compared to anechoic chamber measurements. Also, the ratios between the S_{ii} with A2 stirring (dotted blue curve) and without A2 stirring (dashed red curve), averaged over the frequency bandwidth, are presented in Table I and are denoted $R_{S_{ii}}$. They are close to unity which means that the impact of these variations on the retrieved efficiency is negligible.

The squared modulus of the S-parameters stirred components averaged over the stirrer positions with and without A2 stirring is presented in Fig. 6(a) for $\langle|S_{11,\mathrm{s}}|^2\rangle$, in Fig. 6(b) for $\langle|S_{22,\mathrm{s}}|^2\rangle$ and in Fig. 6(c) for $\langle|S_{21,\mathrm{s}}|^2\rangle$. The R coefficients are computed using the same scheme as for the previous ones, so

TABLE I
R COEFFICIENTS FOR DIFFERENT STIRRING APPROACHES.

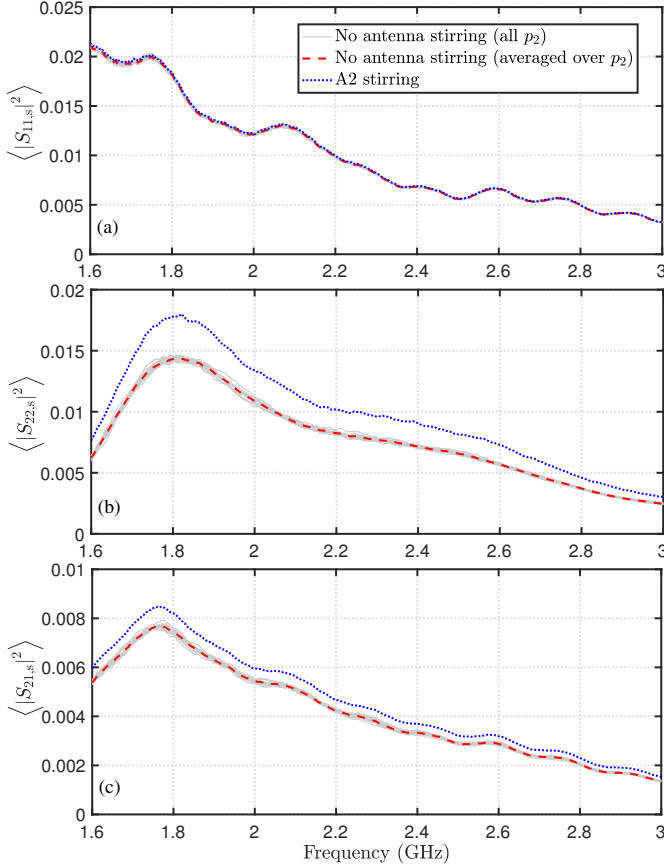|	A2 stirring	A1 stirring	Combined A1-A2 stirring
R_{Q}	1.000	1.000	1.000
$R_{S_{11}}$	1.001	1.007	1.006
$R_{S_{22}}$	1.016	1.004	1.015
$R_{S_{11,\mathrm{s}}}$	1.011	1.122	1.103
$R_{S_{22,\mathrm{s}}}$	1.241	1.076	1.251
$R_{S_{21,\mathrm{s}}}$	1.110	1.111	1.111

Fig. 6. Averaged modulus squared of the stirred components of S_{11} (a), S_{22} (b) and S_{21} (c), as a function of frequency, with and without A2 stirring.

that

$$R_{ij,\mathrm{s}} = \frac{\left\langle \left\langle \left| S_{ij}(\alpha,p_2) - \left\langle \left\langle S_{ij}(\alpha,p_2) \right\rangle_\alpha \right\rangle_{p_2} \right|^2 \right\rangle_\alpha \right\rangle_{p2}}{\left\langle \left\langle \left| S_{ij}(\alpha,p_2) - \left\langle S_{ij}(\alpha,p_2) \right\rangle_\alpha \right|^2 \right\rangle_\alpha \right\rangle_{p_2}}. \quad (8)$$

We observe that on the one hand, the estimation of $\left\langle |S_{11,\mathrm{s}}|^2 \right\rangle$ is not modified by the additional A2 stirring. Indeed, all the estimations are very similar. This indicates that the unstirred component of S_{11} (Fig. 6(a)) is not decreased when performing A2 stirring, i.e., h_{11} in (5) is not modified. This was expected as A1 is not oriented towards A2, which, furthermore, has a small size. On the other hand, we observe that the estimation of $\left\langle |S_{22,\mathrm{s}}|^2 \right\rangle$ (Fig. 6(b)) is strongly modified by A2 stirring. Indeed, it leads to an average relative increase of 24% over the frequency range. This can be understood since the unstirred component of S_{22}, i.e., unstirred by the mechanical
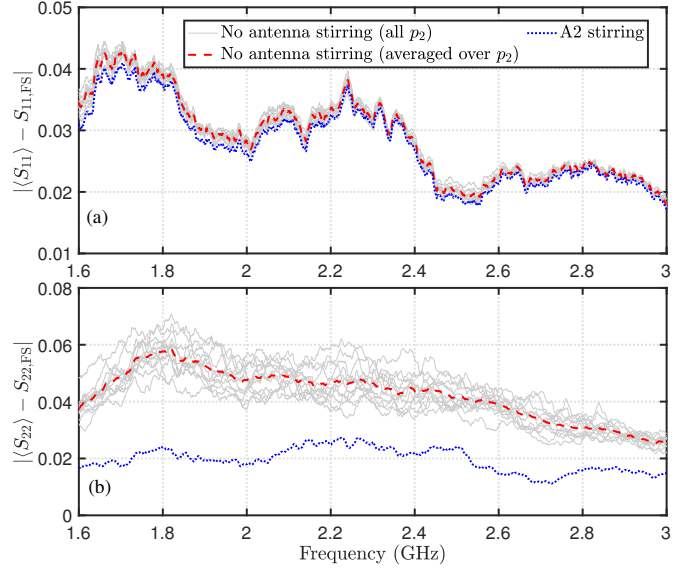

Fig. 7. Error between the average reflection coefficient — S_{11} (a) and S_{22} (b) — measured in the RC and the one measured in the AC as a function of frequency, with and without A2 stirring.

stirring, is modified for each position p_2 so that it is averaged thanks to A2 stirring. The energy that was associated to the unstirred component (represented by h_{22} in (5)) is now taken into account in the stirred component (represented by H_{22} in (5)) and so, the latter increases significantly. Finally, the same behavior is also observed on $\left\langle |S_{21,\mathrm{s}}|^2 \right\rangle$ (Fig. 6(c)) but to a lesser extent. The A2 stirring leads to an average increase of about 11% over the frequency range. Indeed, the transmission coefficient depends on both antenna positions, and the unstirred part of the RC transfer function h_{12} is modified once one antenna is displaced.

As stated in Section II-B, it is classically assumed that a reflection coefficient measured within an RC and averaged over the stirrer positions is equivalent to the FS one, that would be measured in an AC, i.e., that $\left\langle S_{ii}(\alpha) \right\rangle_\alpha = S_{ii,\mathrm{FS}}$. To evaluate the validity of this assumption, we measured the reflection coefficient of both antennas A1 and A2 within the large AC of the ESYCOM laboratory. Then, the modulus of the difference between the RC and the AC measurements is computed as a function of frequency and presented in Fig. 7(a) for the S_{11} and in Fig. 7(b) for the S_{22}, with and without performing A2 stirring. Their average values are presented in Table II. Regarding the S_{11}, the average difference with the one measured in an AC is equal to 0.029, and is slightly lower (5%) when A2 stirring is performed. On the other hand, in the case of S_{22}, this difference is equal to 0.042 on average if no antenna stirring is applied, but strongly decreases thanks to A2 stirring. This demonstrates the necessity to perform antenna stirring in order to reduce the unstirred component of the S-parameters measured within the RC, and thus better evaluate the antenna reflection coefficient.

TABLE II
Modulus of the Difference Between the Reflection
Coefficients Measured Within the RC (Average Over the
Stirring Process) and the AC.

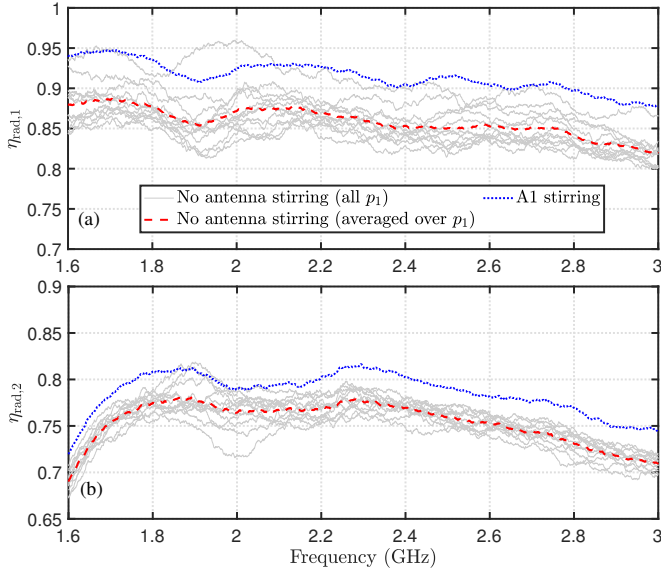|	A2 stirring	A1 stirring	A1-A2 stirring
$\left\|\langle S_{11}\rangle - S_{11,\mathrm{FS}}\right\|$	Without: 0.029 With: 0.028	Without: 0.034 With: 0.017	Without: 0.029 With: 0.011
$\left\|\langle S_{22}\rangle - S_{22,\mathrm{FS}}\right\|$	Without: 0.043 With: 0.020	Without: 0.044 With: 0.039	Without: 0.042 With: 0.020

Fig. 8. Radiation efficiency of A1 (a) and A2 (b) as a function of frequency, with and without A1 stirring.
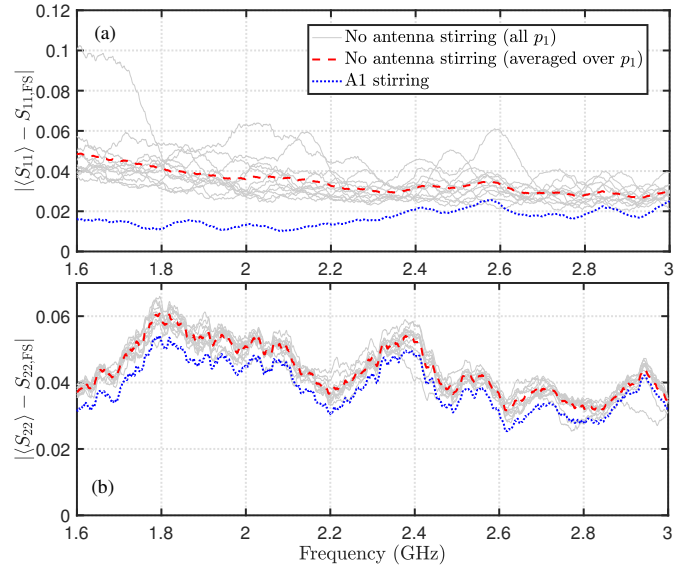

Fig. 9. Error between the average reflection coefficient — S_{11} (a) and S_{22} (b) — measured in the RC and the one measured in the AC as a function of frequency, with and without A1 stirring.

C. A1 Stirring

In this part, we study the influence of A1 stirring on the estimated radiation efficiencies. A2 is thus fixed during the measurement process whereas A1 is moved over the 12 considered positions. The radiation efficiency of A1 is presented in Fig. 8(a) whereas the one of A2 is presented in Fig. 8(b) as a function of frequency. We can see that A1 stirring has a strong impact on the A1 radiation efficiency, which increases by 5.6% on average. This result is coherent with the one obtained with $\eta_{\mathrm{rad},2}$ when applying A2 stirring. However, unlike the results of the previous Section where A2 stirring had no impact on $\eta_{\mathrm{rad},1}$, A1 stirring has also an impact on $\eta_{\mathrm{rad},2}$. Indeed, it increases by 3.2% on average. Therefore, we proceed to the analysis of the evolution of each constitutive parameter of (3) with respect to A1 stirring.

The R coefficients in the case of A1 stirring are presented in the second column of Table I. First of all, R_Q is once again equal to unity, and $R_{S_{11}}$ and $R_{S_{22}}$ are also small enough to be neglected (1.007 and 1.004 respectively). $R_{S_{11},\mathrm{s}}$ is equal to 1.122 which is lower than $R_{S_{22},\mathrm{s}}$ in the A2 stirring case. Indeed, the unstirred component of the log-periodic antenna (A1) oriented directly towards the mechanical mode stirrer is lower than the one from the quasi-omnidirectional A2 antenna, which explains the less significant decrease. $R_{S_{22},\mathrm{s}}$ is quite low (1.076) but much higher than $R_{S_{11},\mathrm{s}}$ for the A2 stirring case. It

means that A1 stirring also significantly decreases the unstirred component of A2. Indeed, A2 being omni-directional, the A1 movement acts as a secondary mode stirrer for A2. A second phenomena occurs: A1 stirring increases the number of RC uncorrelated configurations, which enhances the estimation of the average S_{22} leading to an increase of the A2 radiation efficiency [35]. Finally, $R_{S_{21},\mathrm{s}}$ is very similar to the one obtained using A2 stirring confirming that the movement of one antenna or the other provides a similar stirring regarding the S_{21}.

The difference between the reflection coefficients measured in the RC and in the AC are presented in Fig. 9(a) for S_{11} and in Fig. 9(b) for S_{22}. The average values over the frequency range can be found in Table II. The unstirred component of S_{11} is decreased by a factor of 2 thanks to A1 stirring, whereas the one of S_{22} is slightly decreased (about 13%). These results confirm the aforementioned conclusions.

The movement of each antenna, individually, allows reducing significantly the unstirred component of the reflection coefficient for the moving antenna only. However, the stirred component of both reflection coefficients need to be accurately estimated to accurately retrieve the radiation efficiency of each antenna (3). We can conclude that the movement of both antennas A1 and A2 is required in order to lower the unstirred component of all S-parameters and thus better estimate the radiation efficiency of both antennas. Such experiment is conducted in the next Section.

D. Combined A1-A2 Stirring

In this part, we consider that the two antennas are both moved over the 12 previously considered positions. In order to keep the number of measurements the same, both antennas are moved at the same time in each measurement, which leads to 12 configurations (and 72 stirrer positions for each one). The
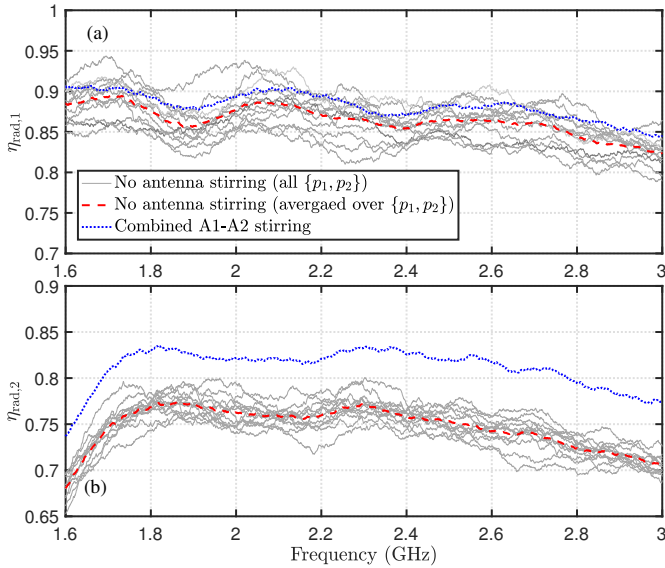
Fig. 10. Radiation efficiency of A1 (a) and A2 (b) as a function of frequency, with and without the combined A1-A2 stirring.
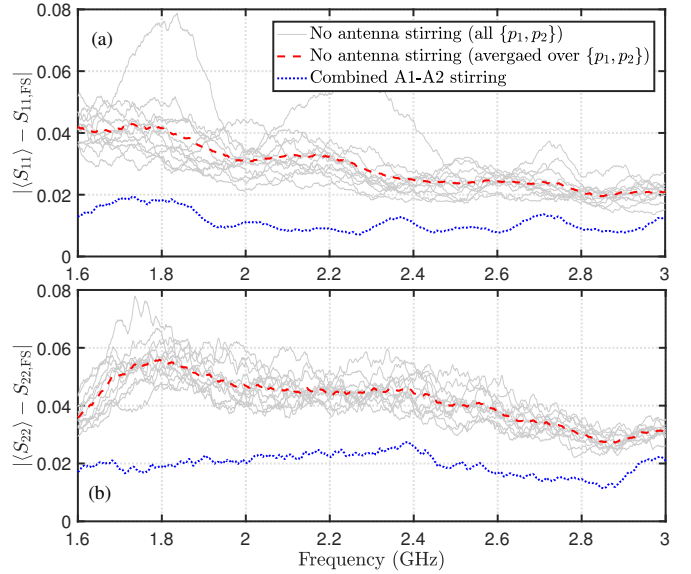

Fig. 11. Error between the average reflection coefficient — S_{11} (a) and S_{22} (b) — measured in the RC and the one measured in the AC as a function of frequency, with and without the combined A1-A2 stirring.

radiation efficiency of antenna A1 is presented in Fig. 10(a) whereas the one of antenna A2 is presented in Fig. 10(b) as a function of frequency. The combined A1-A2 stirring leads to an increase of both radiation efficiency estimations. $\eta_{\mathrm{rad},1}$ increases by 1.8% on average whereas $\eta_{\mathrm{rad},2}$ increases by 6.5% on average. The R coefficients are presented in the third column of Table I. Once again, R_Q is equal to unity, and $R_{S_{11}}$ and $R_{S_{22}}$ are close to unity; therefore, they have a negligible impact on the radiation efficiency increase. Then, $R_{S_{11,\mathrm{s}}}$ is equal to 1.103 which is similar to the value obtained in the A1 stirring case. In the same way, $R_{S_{22,\mathrm{s}}}$ is equal to 1.251 which is very similar to the value obtained in the A2 stirring case. Finally $R_{S_{21,\mathrm{s}}}$ is equal to 1.111 which is almost identical to the two previous cases (A2 stirring, and A1 stirring).

The modulus of the difference between the reflection coefficients measured in the RC and in the AC is presented in Fig. 11(a) for S_{11} and in Fig. 11(b) for S_{22}. and the average differences over the frequency range are presented in the last column of Table II. The combined A1-A2 stirring allows obtaining a lower difference compared to the two other stirring cases for both antennas.

E. Comparison of reflection coefficient results

This part focuses on a comparison between all RC reflection coefficient measurements with respect to the ones obtained in an AC (Table II). Without antenna stirring, the error is lower for A1. Indeed, on the one hand, A1 is a directional antenna oriented towards the mechanical stirrer (not facing a flat wall); therefore, direct reflections towards A1 are limited. On the other hand, A2 is an omni-directional antenna and therefore, it is possibly subjected to higher unstirred components due to direct reflections upon flat walls in some directions. This could explain the lower error level in the case of A1 than the case of A2 in this specific set-up. The A2 stirring has a strong impact on A2 reflection coefficient and a negligible one on A1

reflection coefficient. Indeed, A1 is not oriented towards A2 so that A2 does not modify the A1 reflection coefficient. The A1 stirring has a strong impact on A1 reflection coefficient and a less one, but not negligible, on A2 reflection coefficient. Indeed, A2 being omni-directional, it is sensitive to the A1 position that acts as a moving scatterer. Finally, the combined A1-A2 stirring allows reducing both errors by a factor of 3 in the case of A1 and a factor of 2 in the case of A2.

F. Comparison of radiation efficiency results

To summarize all the efficiency results presented in the previous parts, a comparison between all the conducted measurements is made. More specifically, it compares the radiation efficiency of both antennas in the case of 1) no antenna stirring, 2) A1 stirring, 3) A2 stirring and 4) combined A1-A2 stirring. The A1 radiation efficiency is presented in Fig. 12 as a function of frequency. It is observed that A2 stirring has no impact on $\eta_{\mathrm{rad},1}$. This can be explained as the unstirred component of S_{11} remains the same (A1 is never oriented towards A2), whereas the increases of the estimated stirred components of S_{22} and S_{21} compensate each other in (3). The A1 stirring leads to a 7.0% increase on average. In this case, the unstirred component of S_{11} is strongly reduced (thus, the stirred component of S_{11} is strongly increased), whereas the one of S_{22} remains unchanged. Finally, the combined A1-A2 stirring leads to a moderate increase of 3.8% on average. In this case, the effect on the estimation of $S_{21,\mathrm{s}}$ is similar to the previous two cases as the unstirred component of S_{21} is strongly reduced once the position of at least one antenna is modified. However, the unstirred components of both reflection coefficients are strongly reduced. The hypothesis that the S-parameters averaged over the stirring process is equal to the FS one is better verified for the combined A1-A2 stirring (see Table II).
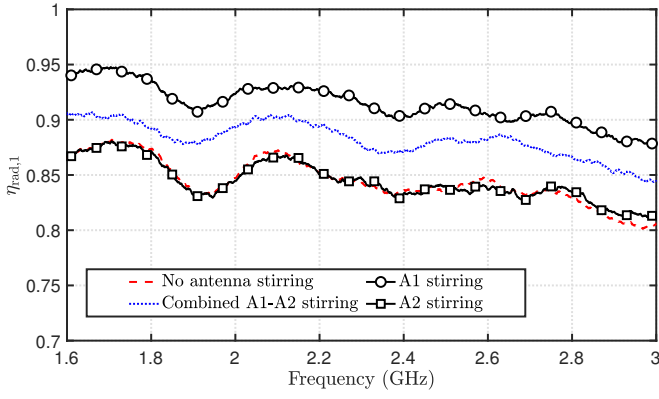
Fig. 12. A1 radiation efficiency as a function of frequency for different stirring approaches.

Fig. 14. A1 radiation efficiency as a function of frequency for different stirring approaches, estimated in the larger RC.
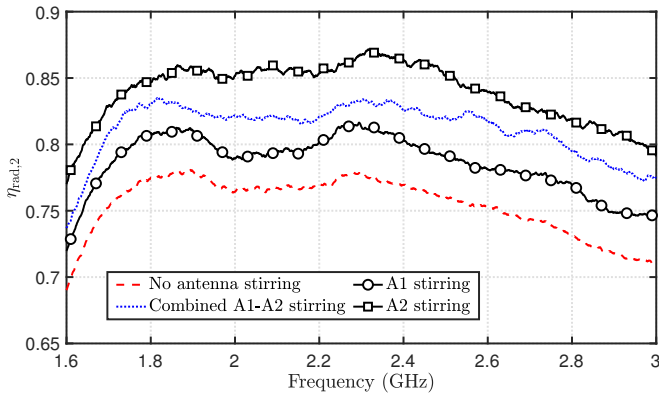

Fig. 13. A2 radiation efficiency as a function of frequency for different stirring approaches.

Similar conclusions can be drawn from the A2 radiation efficiency presented in Fig. 13 as a function of frequency. However, in this case, even A1 stirring has an impact on $\eta_{\text{rad},2}$, which leads to a 3.2% increase. Indeed, antenna A2 is omni-directional and its reflection coefficient is thus sensitive to the location of A1 (which is furthermore of significant size). Therefore, A1 acts as a scatterer within the RC and contributes to the decrease of the unstirred component of S_{22} (about 13%) in addition to generating additional uncorrelated RC configurations. Apart from this, the less biased estimation, obtained with the combined A1-A2 stirring, corresponds to a 5.8% increase on average compared to the value without any antenna stirring. The A2 stirring leads to a radiation efficiency overestimation of 2.8% whereas A1 stirring leads to a radiation efficiency underestimation of 2.6%.

IV. IMPACT OF THE RC SIZE

In this section, we aim at emphasizing the impact of the RC size, hence Q-factor, on the retrieved results. Another experiment has been performed in the same 1.6 to 3 GHz frequency range in the large RC of IETR (93 m^3) also equipped with a rotating mechanical mode stirrer. A1 is the same log-periodic antenna whereas A2 is a wideband patch antenna (different from the one in the previous section). In addition to 72 stirrer positions, the same antenna stirring
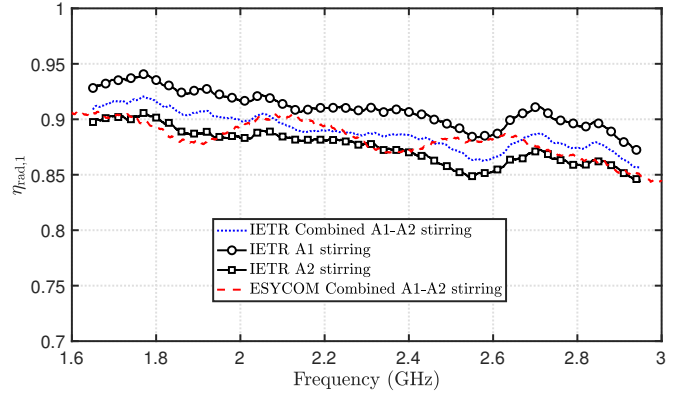
processes are performed here: 1) 12 A1 positions, 2) 12 A2 positions, and 3) 12 combined A1-A2 positions. The Q-factor varies from 26,000 to 50,000 in the frequency range, making it between 3.8 and 4.5 times higher than the one in the previous measurements. Also, all stirrer positions can be considered as uncorrelated so that $N_{\text{eff}} = 72$ around the central frequency [33], which is about three times higher than the case of previous measurements.

For brevity, we present directly the radiation efficiencies averaged over the three stirring cases for the log-periodic antenna only (Figure 14). Three main conclusions can be drawn. Firstly, the same phenomenon regarding the biased estimation is observed. Indeed, A1 stirring (i.e., platform stirring only) leads to an overestimation of the radiation efficiency whereas A2 stirring (i.e., source stirring only) leads to an underestimation of the antenna radiation efficiency. Secondly, the bias is reduced compared to the previous measurements. Indeed, the average absolute difference between the two biased estimations is equal to 3.4% whereas it was equal to 5.3% in the previous measurement. This can be explained by the much larger size of the RC, implying antennas being located further away from the walls and thus less likely to exhibit unstirred components. Thirdly, it can be seen that the radiation efficiency estimated for the combined A1-A2 stirring is in very good agreement with the one obtained in the previous measurement in the RC of ESYCOM. Indeed, the average absolute difference between the two is equal to only 1.18% with a maximum error of 2.96%.

V. CONCLUSION

In this paper, we have shown that the antenna stirring of both antennas is required in order to obtain an unbiased estimation of the antenna radiation efficiency using the two-antenna method within an RC. Antenna stirring is used here to refer to both platform stirring (which usually refers to the AUT stirring only) and source stirring (which refers to the source antenna, i.e., the other measurement antenna). Indeed, the mechanical stirring is mandatory to ensure enough uncorrelated RC configurations, but fails at vanishing the unstirred components of the S-parameters that are due to the direct reflections between the antennas and the walls or

any standing objects within the RC. As a consequence, the stirred components of the S-parameters, whose evaluation is shown to be crucial to retrieve the antenna radiation efficiency, are underestimated. This leads to either an overestimation of A2 (A1) radiation efficiency if only A2 stirring (A1 stirring) is performed, or an underestimation of A2 (A1) radiation efficiency if only A1 stirring (A2 stirring) is performed.

We highlighted that the evaluation of the stirred component of the transmission coefficient benefits equally from any antenna stirring, since the unstirred component is modified as soon as one antenna is moved. However, the evaluation of the stirred components of the reflection coefficients of both antennas needs to be properly estimated, thus requiring the movement of both antennas.

It is also shown that, in our particular setup, the directional antenna (A1) is less sensitive to the antenna stirring than the omni-directional one (A2). Indeed, A1 being both directional and oriented towards the mechanical mode stirrer may explain the lower level of unstirred paths with respect to the A2 antenna facing flat walls and being isotropic. However, this deserves further investigations.

It has to be noted that although the current results are obtained using the two-antenna approach, most RC measurement techniques to retrieve antenna radiation efficiency are based on the evaluation of the stirred components of S-parameters and would therefore also benefit from a combined antenna stirring.

Acknowledgements

References

[1] J. G. Andrews, S. Buzzi, W. Choi, S. V. Hanly, A. Lozano, A. C. K. Soong, and J. C. Zhang, "What will 5g be?" IEEE J. Sel. Areas Commun., vol. 32, no. 6, pp. 1065–1082, 2014.

[2] A. Ghosh, A. Maeder, M. Baker, and D. Chandramouli, "5g evolution: A view on 5g cellular technology beyond 3gpp release 15," IEEE Access, vol. 7, pp. 127 639–127 651, 2019.

[3] M. Chen, Y. Miao, Y. Hao, and K. Hwang, "Narrow band internet of things," IEEE Access, vol. 5, pp. 20 557–20 577, 2017.

[4] F. Sarrazin, S. Pflaum, and C. Delaveaud, "Radiation efficiency improvement of a balanced miniature ifa-inspired circular antenna," IEEE Antennas Wireless Propag. Lett., vol. 16, pp. 1309–1312, 2017.

[5] C. A. Balanis, Antenna theory: analysis and design. Wiley-Interscience, 2005.

[6] H. A. Wheeler, "The radiansphere around a small antenna," Proc. IRE, vol. 47, no. 8, pp. 1325–1331, 1959.

[7] M.-C. Huynh, "Wideband compact antennas for wireless communication applications," 2004.

[8] G. Le Fur, C. Lemoine, P. Besnier, and A. Sharaiha, "Performances of uwb wheeler cap and reverberation chamber to carry out efficiency measurements of narrowband antennas," IEEE Antennas Wireless Propag. Lett., vol. 8, pp. 332–335, 2009.

[9] J. Rosengren and K. Carlsson, "Measurements of terminal antennas performance in multimode reverberation chambers," 2000.

[10] M. Piette, "Antenna radiation efficiency measurements in a reverberation chamber," in Proc. Asia-Pacific Radio Sci. Conf., Aug 2004, pp. 19–22.

[11] P. Besnier, J. Sol, A. Presse, C. Lemoine, and A. C. Tarot, "Antenna efficiency measurement from quality factor estimation in reverberation chamber," in 46th Europ. Microw. Conf. (EuMC), Oct 2016, pp. 715–718.

[12] C. L. Holloway, H. A. Shah, R. J. Pirkl, W. F. Young, D. A. Hill, and J. Ladbury, "Reverberation chamber techniques for determining the radiation and total efficiency of antennas," IEEE Trans. Antennas Propag., vol. 60, no. 4, pp. 1758–1770, April 2012.

[13] Q. Xu, Y. Huang, X. Zhu, L. Xing, Z. Tian, and C. Song, "A modified two-antenna method to measure the radiation efficiency of antennas in a reverberation chamber," IEEE Antennas Wireless Propag. Lett., vol. 15, pp. 336–339, 2016.

[14] W. Krouka, F. Sarrazin, J. d. Rosny, A. Labdouni, and E. Richalot, "Antenna radiation efficiency estimation from backscattering measurement performed within reverberation chambers," IEEE Trans. Electromagn. Compat., pp. 1–8, 2021.

[15] R. Serra, A. C. Marvin, F. Moglie, V. M. Primiani, A. Cozza, L. R. Arnaut, Y. Huang, M. O. Hatfield, M. Klingler, and F. Leferink, "Reverberation chambers a la carte: An overview of the different mode-stirring techniques," IEEE Electromagn. Compat. Mag., vol. 6, no. 1, pp. 63–78, 2017.

[16] Y. Huang and D. Edwards, "A novel reverberating chamber: The source-stirred chamber," in Int. Conf. Electromagn. Compat., 1992, pp. 120–124.

[17] Q. Xu, L. Xing, Y. Zhao, T. Jia, and Y. Huang, "A source stirred reverberation chamber using a robotic arm," IEEE Trans. Electromagn. Compat., vol. 62, no. 2, pp. 631–634, 2020.

[18] V. M. Primiani, P. Russo, and G. Cerri, "Design and testing of an antenna system for the source stirring technique in reverberation chambers," J. Electromagn. Waves Appl., vol. 26, pp. 837 – 850, 2012.

[19] A. De Leo, G. Cerri, P. Russo, and V. Mariani Primiani, "Experimental comparison between source stirring and mechanical stirring in a reverberation chamber by analyzing the antenna transmission coefficient," in Int. Symp. Electromagn. Compat. (EMC EUROPE), 2018, pp. 677–682.

[20] P.-S. Kildal and C. Carlsson, "Detection of a polarization imbalance in reverberation chambers and how to remove it by polarization stirring when measuring antenna efficiencies," Microw. Opt. Tech. Lett., vol. 34, no. 2, pp. 145–149, 2002. [Online]. Available: https://onlinelibrary.wiley.com/doi/abs/10.1002/mop.10398

[21] K. Rosengren, P.-S. Kildal, C. Carlsson, and J. Carlsson, "Characterization of antennas for mobile and wireless terminals by using reverberation chambers: Improved accuracy by platform stirring," in IEEE Int. Symp. Antennas Propag. Soc., vol. 3, 2001, pp. 350–353 vol.3.

[22] P.-S. Kildal, S.-H. Lai, and X. Chen, "Direct coupling as a residual error contribution during ota measurements of wireless devices in reverberation chamber," in IEEE Int. Symp. Antennas Propag. Soc., 2009, pp. 1–4.

[23] P. Kildal, C. Carlsson, and J. Yang, "Measurement of free-space impedances of small antennas in reverberation chambers," Microw. Opt. Tech. Lett., vol. 32, pp. 112–115, 2002.

[24] W. Krouka, F. Sarrazin, and E. Richalot, "Influence of the reverberation chamber on antenna characterization performances," in 2018 Int. Symp. Electromagn. Compat. (EMC EUROPE), 2018, pp. 329–333.

[25] W. Krouka, F. Sarrazin, J. Sol, P. Besnier, and E. Richalot, "Comparison of antenna radiation efficiency measurement techniques in reverberation chamber using or not a reference antenna," in Europ. Conf. Antenna Propag. (EuCAP), Mar 2020.

[26] A. Hubrechsen, K. A. Remley, R. D. Jones, D. F. Williams, D. Gu, A. B. Smolders, and L. A. Bronckers, "The effect of noise on reverberation-chamber measurements of antenna efficiency," IEEE Trans. Antennas Propag., pp. 1–1, 2021.

[27] J. M. Ladbury and D. A. Hill, "An improved model for antennas in reverberation chambers," in IEEE Int. Symp. Electromagn. Compat., 2010, pp. 663–667.

[28] C. Li, T. Loh, Z. Tia, Q. Xu, and Y. Huang, "Evaluation of chamber effects on antenna efficiency measurements using non-reference antenna methods in two reverberation chambers," in IET Microwaves, Antennas & Propagation, vol. 11, no. 11, 2017, pp. 1536–1541.

[29] P. Besnier, J. Sol, and S. Mric, "Estimating radar cross-section of canonical targets in reverberation chamber," in Int. Symp. Electromagn. Compat. (EMC EUROPE), 2017, pp. 1–5.

[30] A. Reis, F. Sarrazin, P. Pouliguen, J. Sol, P. Besnier, and E. Richalot, "Radar cross section measurement within reverberation chamber: Stirrer position issues," in Europ. Conf. Antennas Propag. (EuCAP), 2020, pp. 1–4.

[31] A. Reis, F. Sarrazin, E. Richalot, S. Mric, J. Sol, P. Pouliguen, and P. Besnier, "Radar cross-section pattern measurements in a mode-stirred reverberation chamber: Theory and experiments," IEEE Trans. Antennas Propag., vol. 69, no. 9, pp. 5942–5952, 2021.

[32] A. Reis, F. Sarrazin, P. Besnier, P. Pouliguen, and E. Richalot, "Contactless antenna gain pattern estimation from backscattering coefficient

measurement performed within reverberation chambers," IEEE Trans. Antennas Propag., 2021.

[33] C. Lemoine, P. Besnier, and M. Drissi, "Estimating the effective sample size to select independent measurements in a reverberation chamber," IEEE Trans. Electromagn. Compat., vol. 50, no. 2, pp. 227–236, 2008.

[34] L. Bronckers, A. Roc?h, and A. Smolders, "Reverberation chamber enhanced backscattering: High-frequency effects," in 2019 Int. Symp. Electromagn. Compat. - EMC EUROPE, 2019, pp. 1–6.

[35] X. Chen, "On statistics of the measured antenna efficiency in a reverberation chamber," IEEE Trans. Antennas Propag., vol. 61, no. 11, pp. 5417–5424, 2013.